

Collective dynamics of the p-Pb collisions at the LHC

WOJCIECH BRONIEWSKI^{1,2}, PIOTR BOŻEK^{2,3}

¹ Institute of Physics, Jan Kochanowski University, 25-406 Kielce, Poland

² The H. Niewodniczański Institute of Nuclear Physics, Polish Academy of Sciences, 31-342 Kraków, Poland

³ AGH University of Science and Technology, Faculty of Physics and Applied Computer Science, 30-059 Krakow, Poland

We review the signatures for the soft collective dynamics in highest-multiplicity ultrarelativistic p-Pb collisions and show that the effects are well described in a three-stage model, consisting of the event-by-event Glauber initial conditions, viscous 3+1D hydrodynamics, and statistical hadronization. In particular, we discuss the ridges in two-particle correlations in the relative azimuth and pseudorapidity, the elliptic and triangular flow coefficients, and the mass hierarchy of observables sensitive to flow.

1. Introduction

This talk is based on Refs. [1–3], where the details and more complete lists of references can be found (see also the mini-review [4]). We wish to address here the most intriguing physics questions concerning the topic:

- Are the highest-multiplicity p-Pb collisions *collective*?
- What is the nature of the initial state and correlations therein?
- What are the limits in conditions on applicability of hydrodynamics?

Recall that the *collective flow* is one of the principal signatures of the strongly-interacting Quark-Gluon Plasma formed in ultra-relativistic A-A collisions at RHIC and the LHC. It manifests itself in harmonic components in the momentum spectra v_n , in specific structures in the correlation data (*ridges*), in *mass hierarchy* of the p_T spectra and v_n 's of identified particles, as well as in certain features of interferometry (femtoscopy). Since 1) the ridges were found experimentally at the LHC in p-Pb collisions [5], 2) large elliptic and triangular flow was measured in p-Pb [5], 3) strong mass hierarchy was recently detected in p-Pb [6], there are clear analogies between the “collective” A-A system and the “small” p-A system. Below we present

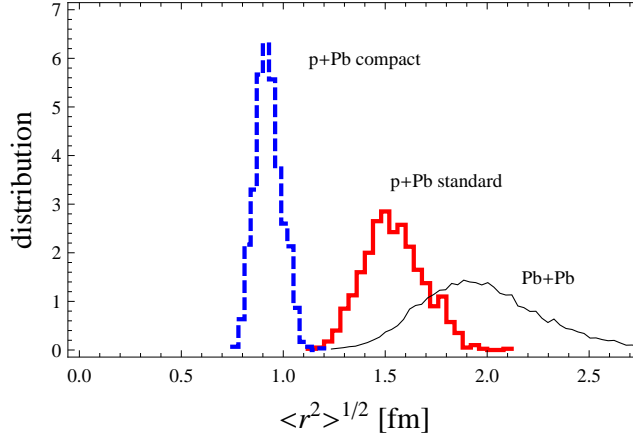


Fig. 1. Event-by-event distribution of the rms size of the Glauber initial conditions for the *fixed* number of participants, $N_p = 18$, for the standard source in p-Pb (thick solid line) obtained by placing the sources at the centers of participants, the compact source (dashed line), obtained by placing the sources in the center-of-mass of the colliding pair [10], and for the peripheral Pb-Pb collisions (thin solid line). The p-Pb sizes are not more that twice smaller from the Pb-Pb sizes. At the same time, the p-Pb system is more dense. This allows to analyze the p-Pb system with viscous hydrodynamics [4].

the evidence for the collective interpretation of the highest-multiplicity p-A collisions.

2. Three-stage approach

To place our argumentation on a quantitative level, we use the three stage approach consisting of 1) modeling of the initial phase with the Glauber approach as implemented in GLISSANDO [7], 2) applying event-by-event 3+1D viscous hydrodynamics [8] to the intermediate evolution, and 3) carrying out statistical hadronization at freezeout with THERMINATOR [9]. The details can be found in Refs. [1, 2]. Here we only wish to point out the similarity of the initial conditions in high-multiplicity p-A collisions to those in peripheral A-A collisions, as seen from Fig. 1. This indicates that our approach should work with similar accuracy for the most central p-Pb collisions as it worked for the Pb-Pb collisions at centralities $\sim 70\%$.



Fig. 2. Creation of the near-side ridge: The surfers' motion is correlated even when they are widely separated along the shore.

3. The ridge

The emergence of the ridges in the two-particle correlations in the relative azimuth and pseudorapidity, $C(\Delta\eta, \Delta\phi) = N_{\text{phys}}^{\text{pairs}}(\Delta\eta, \Delta\phi) / N_{\text{mixed}}^{\text{pairs}}(\Delta\eta)$, finds a natural explanation in correlated collective flow orientation within a long pseudorapidity span. This is cartooned in Fig. 2. Numerical calculation in our approach yields fair agreement with the data, as indicated in Fig. 3, providing alternative explanation to the color-glass approach [11]. As shown below, the event-by-event hydrodynamics also yields the proper magnitude of the triangular component of the flow in a natural way.

4. Harmonic flow

The structure of the correlation data (similar to the top panel of Fig. 3) indicates that one may get rid of most of the nonflow effects by excluding the central peak from the analysis, simply using pairs with $|\Delta\eta| > 2$. The flow coefficients ($v_n\{2, |\Delta\eta| > 2\}$) obtained that way from the experiment and from our model simulations are compared in Figs. 4 and 5. We note a very fair agreement with the data for the highest-multiplicity events. As the system becomes smaller, the simulations depart from the experiment, indicating that the dissipative effects or the direct production from the corona are becoming important.

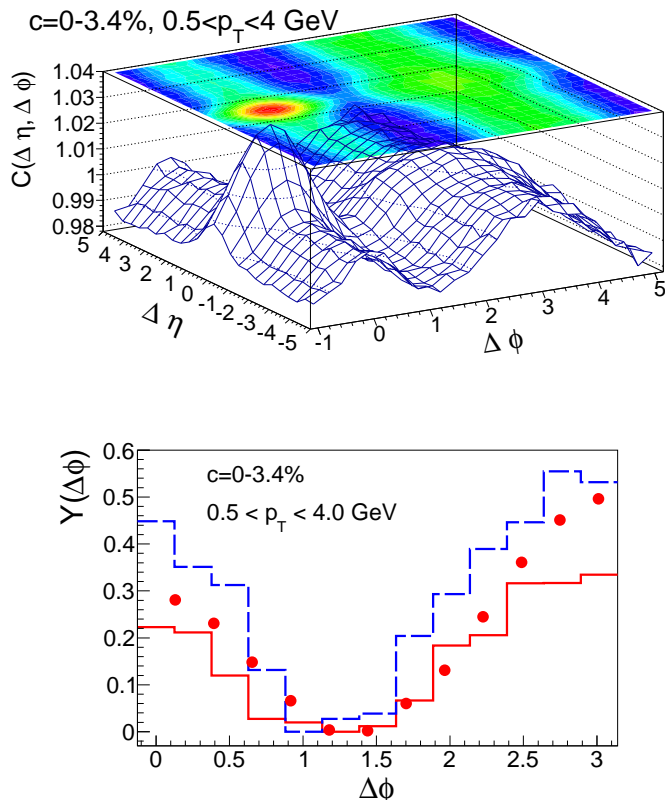


Fig. 3. Correlation functions in the ATLAS kinematic conditions. Top: $C(\Delta\phi, \Delta\eta)$. Bottom: the projected ($2 \leq |\Delta\eta| \leq 5$) per-trigger correlation function $Y(\Delta\phi) = \int B(\Delta\phi)d(\Delta\phi)C(\Delta\phi)/N - b_{ZYAM}$, compared to the ATLAS data. The solid (dashed) lines correspond to the standard (compact) source.

5. Mass hierarchy

A very important effect of the presence of collective flow is the emergent mass hierarchy in certain heavy-ion observables [3, 12]. The effect is kinematic: hadrons emitted from a moving fluid element acquire more momentum when they are more massive. For that reason, for instance, the average transverse momentum of the protons is significantly higher than for the kaons, which in turn is higher than for the pions. The results, showing agreement of our approach with the data, are presented in Fig. 6(a). As a benchmark with no flow, we show in Fig. 6(b) the results of the HIJING simulations, exhibiting much smaller splitting.

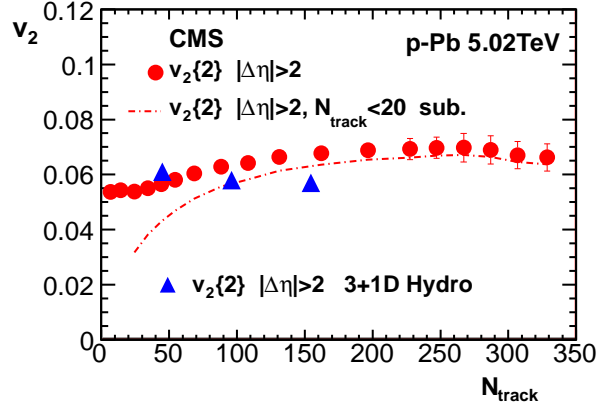


Fig. 4. The elliptic flow coefficient $v_2\{2, |\Delta\eta| > 2\}$ from our model (points) compared to the CMS data.

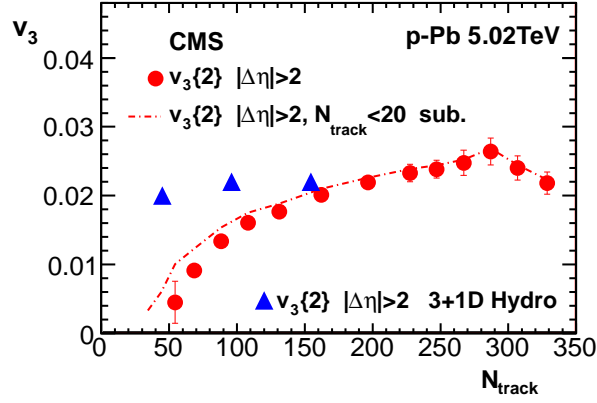


Fig. 5. Same as Fig. 4 but for the triangular flow $v_3\{2, |\Delta\eta| > 2\}$. The departure of the model from the experiment for lower centrality classes indicates the limits of validity of the collective approach.

A proper pattern in the differential identified-particle elliptic flow is also found, as seen from Fig. 7. We note that a very general argument in favor of collectivity, based on failure of superposition in the p-A spectra, has been brought up in Ref. [13].

6. Conclusions

The numerous experimental data from the LHC for the p-Pb collisions of highest multiplicity are compatible with the collective expansion scenario: the formation of the two ridges, large elliptic and triangular flow, and the mass hierarchy found in the average transverse momentum and in the differential elliptic flow [3, 12]. Thus the p-Pb system can be used as a test

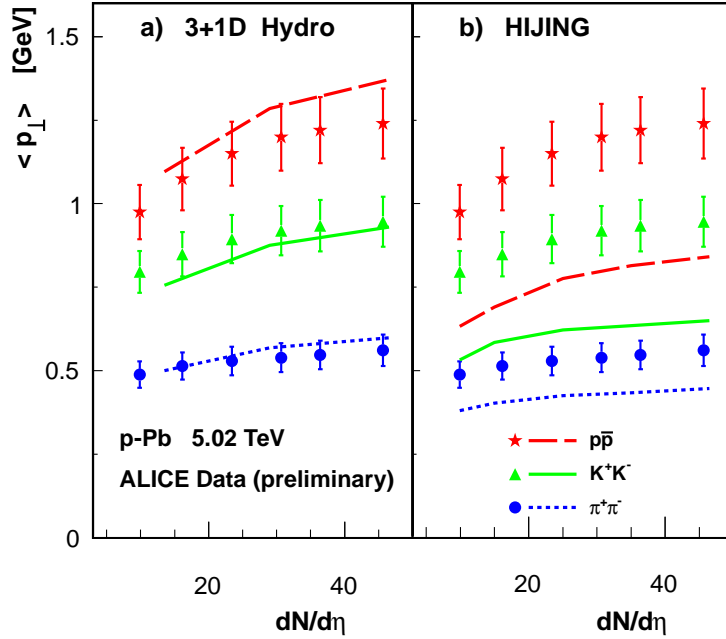


Fig. 6. Mean transverse momentum of identified particles produced in the p-Pb collisions, plotted as a function of the charged particle density. (a) our model, and for comparison (b) HIJING 2.1, where no collective effects are present. The lines correspond to the model calculations, while the data points come from Ref. [6].

ground for the onset of collective dynamics. Certainly, lower multiplicity events are “contaminated” with other effects, e.g., the production from the corona nucleons and their modeling must be more involved. Another signature of collectivity would be provided by the interferometric radii, where the model calculation for p+Pb place the results closer to the A+A lines and farther from the p+p lines [14].

Acknowledgments

This work was supported by the Polish National Science Centre, grants DEC-2012/06/A/ST2/00390 and DEC-2011/01/D/ST2/00772, and PL-Grid infrastructure.

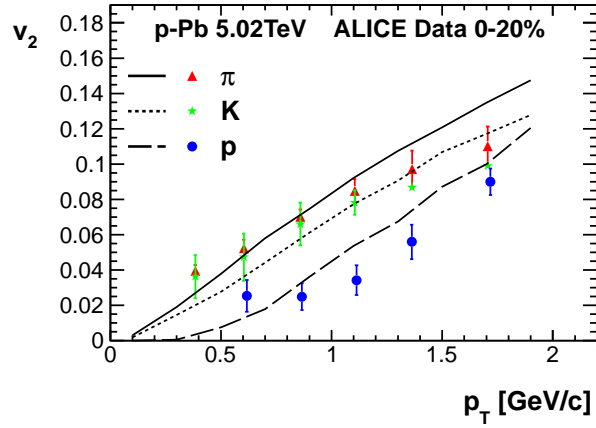


Fig. 7. $v_2\{2\}$ for pions, kaons and protons in p-Pb collisions calculated in our model, plotted as a function of the transverse momentum. The data come from Ref. [6].

REFERENCES

- [1] P. Bożek and W. Broniowski, Phys. Lett. **B718**, 1557 (2013), 1211.0845.
- [2] P. Bożek and W. Broniowski, Phys. Rev. **C88**, 014903 (2013), 1304.3044.
- [3] P. Bożek, W. Broniowski, and G. Torrieri, Phys.Rev.Lett. **111**, 172303 (2013), 1307.5060.
- [4] P. Bożek, W. Broniowski, and G. Torrieri (2013), 1309.7782.
- [5] S. Chatrchyan et al. (CMS Collaboration), Phys. Lett. **B718**, 795 (2013), 1210.5482.
 B. Abelev et al. (ALICE Collaboration), Phys.Lett. **B719**, 29 (2013), 1212.2001.
 G. Aad et al. (ATLAS Collaboration), Phys.Rev.Lett. **110**, 182302 (2013), 1212.5198.
 G. Aad et al. (ATLAS Collaboration), Phys.Lett. **B725**, 60 (2013), 1303.2084.
 S. Chatrchyan et al. (CMS Collaboration), Phys.Lett. **B724**, 213 (2013), 1305.0609.

- [6] S. Chatrchyan et al. (CMS Collaboration) (2013), 1307.3442.
B. B. Abelev et al. (ALICE Collaboration), Phys.Lett. **B726**, 164 (2013), 1307.3237.
B. B. Abelev et al. (ALICE Collaboration) (2013), 1307.1094.
- [7] W. Broniowski, M. Rybczyński, and P. Bożek, Comput. Phys. Commun. **180**, 69 (2009), 0710.5731.
M. Rybczynski, G. Stefanek, W. Broniowski, and P. Bozek (2013), 1310.5475.
- [8] P. Bożek, Phys. Rev. **C85**, 034901 (2012), 1110.6742.
- [9] A. Kisiel, T. Tałuć, W. Broniowski, and W. Florkowski, Comput. Phys. Commun. **174**, 669 (2006), nucl-th/0504047.
M. Chojnacki, A. Kisiel, W. Florkowski, and W. Broniowski, Comput. Phys. Commun. **183**, 746 (2012), 1102.0273.
- [10] A. Bzdak, B. Schenke, P. Tribedy, and R. Venugopalan, Phys. Rev. **C87**, 064906 (2013), 1304.3403.
- [11] K. Dusling and R. Venugopalan, Phys.Rev.Lett. **108**, 262001 (2012), 1201.2658.
K. Dusling and R. Venugopalan, Phys. Rev. **D87**, 094034 (2013), 1302.7018.
- [12] K. Werner, M. Bleicher, B. Guiot, I. Karpenko, and T. Pierog (2013), 1307.4379.
- [13] A. Bzdak and V. Skokov, Phys.Lett. **B726**, 408 (2013), 1306.5442.
- [14] P. Bożek and W. Broniowski, Phys. Lett. **B720**, 250 (2013), 1301.3314.